

Experimental Investigations of Porosity and Permeability of Flocs in the Suspensions of Biological Water Treatment Plants

Boštjana Žajdela^{1*}, Matjaž Hriberšek², Aleš Hribernik²

¹ Regionalna razvojna agencija Mura, Slovenia

² Univerza v Mariboru, Fakulteta za strojništvo, Slovenia

This paper deals with the movement of flocs in suspension, as they appear in biological wastewater treatment (BWT) plants. Basic equations for solving the problem and analysis of wastewater composition of BWT plant Lendava are presented. Greater attention is given to the geometrical and sedimentation characteristics of solid flocs, key parameters for developing a fast numerical procedure for simulating flocs' movements. An extensive analysis regarding floc size distribution and settling velocity is presented. Based on the results of experimental investigations, the main physical parameters of the flocs are defined and calculated by considering floc porosity.

© 2008 Journal of Mechanical Engineering. All rights reserved.

Keywords: wastewater treatment, biological treatment plants, sedimentation, permeability

1 DESCRIPTION OF PROBLEM

Monitoring and predicting processes within multiphase compounds, when acting as working material in biological wastewater treatment plants, is closely linked to understanding the phenomena relating to transfer, such as the transfer of momentum, heat and mass. In regard to those processes running within biological wastewater treatment plants, the most common forms of multiphase systems are solid-liquid and solid-liquid-gas. The impact of solid particles on transfer processes in such systems is, therefore, one of the key factors needing to be considered in order to provide an accurate description of processes within biological wastewater treatment plants. Solid impurities of either organic (algae, bacteria, remains of dead organisms) or inorganic (clay, silt, soil, mud, sand) origins are normally heavier than water. Sedimentation in the sedimentation pool is intended for clearing the wastewaters of suspended mass with density higher than those of the surrounding water. Particle movement accelerates for as long as form resistance and liquid friction forces at the particle's surface do not equal the gravity and buoyancy. Form resistance is normally considerably higher than friction resistance, thus allowing for the latter to be ignored.

Considerable influence on sedimentation duration is exercised by the sludge flocs' shapes (influencing the drag coefficient), the sizes of primary particles and sludge flocs, the permeability of sludge flocs and their densities. These parameters are also important when modelling the flocs' sedimentation.

In earlier work [1] we paid greater attention to determining the size distributions and main geometrical parameters of the sludge flocs, by means of image analysis. Additionally, free-settling tests were used in connection with empirical models for determining drag coefficient (C_d), in order to evaluate the flocs' densities.

Image analysis is often used for size analysis. Li and Ganczarzyk [2] and [3] used image analysis to examine the size distributions and internal structures of activated sludge flocs. Their work focused on automated image analysis for characterizing sludge settling properties and to obtain sludge concentration data.

The internal structure of an activated sludge floc is porous. Flocs are composed of several primary particles. Lee et. al. [4] estimate that the diameter of primary particles is between 1 and 20 μm . Li and Ganczarzyk [2] arbitrarily took d_p as between 1 and 10 μm and they used the 2 μm diameter of a primary particle for permeability porosity correlations. Also Huang [5] determined that the size of a primary particle's

*Corr. Author's Address: Boštjana Žajdela, Regionalna razvojna agencija Mura, Slovenia
boštjana.zajdela@rra-mura.si

diameter is smaller than 10 μm . Jorand et al. [6] analysed floc structure, which was obtained by breaking-down activated sludge flocs using ultrasound. They established that in activated sludge flocs the predominating macroflocs size was 125 μm . These are formed from 13 μm microfloc aggregates, which are made up of smaller particles of size 2.5 μm .

Floc porosity does not only influence their density; it also enables internal permeation of liquid through particles. In practice this fact is often neglected [7] and [8], although research into this theme does exist. Floc porosity according to Huang [5] increases (density decreases) as floc size increases. Lee et al. [4] came to the same conclusions when investigating settling activated by drilling sludge floc from a sea's bottom. They state that permeability might change from 10^{-17} to 10^{-8} m^2 . Mutsumoto and Suganuma [9] experimentally researched the effect of permeability on the settling velocity of a porous sphere by using a permeable model floc made of steel wool and ascertained that the effect of permeability on a model floc's settling velocity can be neglected at lower values. Li and Yuan [10] presented data on the permeability of microbial aggregates for an activated sludge treatment plant and ascertain that flocs (1.0 – 2.5 mm) are porous and fractal. Here settling velocities were only slightly higher as those predicted by Stoke's law for identical but impermeable particles. Microbial aggregates could have largely reduced permeability, as the pores between the microorganisms in the aggregates may be clogged.

In most studies, ρ_p density of primary particle, is assumed to be equal to the dry density of aggregate ρ_{SS} [7] and [11], which is true if the primary particle does not contain liquid. Li and Yuan [10] observed the settling of activated sludge in liquid of different densities, and ascertained that the density of an individual cell (primary particle) is 1.059 g/cm^3 . Lee et al. [4] used a free-settling test for estimating activated sludge floc density. Their estimation was obtained on the basis of a single floc's terminal velocity and its diameter.

This paper describes a procedure for defining those floc characteristics that influence the course of interaction with the liquid phase and are necessary for numerical modelling of floc sedimentation. By processing images, taken

through a microscope, and recording floc projections at three basic levels, we calculated the volumes of the flocs and evaluated their morphological characteristics. Then the flocs were recorded during free sedimentation and the images processed using software which defined the sizes of flocs and their locations on the images. By considering the time-interval between two successive shots (0.75 s), it was possible to calculate the flocs sedimentation velocities. The experimentally defined results were used to develop empirical models for porosities and densities of flocs.

2 FLOC SEDIMENTATION MODELLING

2.1 Basic Equations

Floc sedimentation can be simulated using a simplified model of force balance for a floc:

$$m_k \frac{d\bar{v}_k}{dt} = -\frac{1}{8} \pi \rho_l d_k^3 \Omega C_d |\bar{v}_k - \bar{v}_i| (\bar{v}_k - \bar{v}_i) + \frac{1}{6} \pi d_k^3 (\rho_k - \rho_l) g \quad (1)$$

this model considers inertial force and dynamic buoyancy, the other forces being ignored as previous research has shown [1] that Reynolds number values are $(Re) < 3$. This ensures that the importance of drag coefficient (C_d), comprising the flow characteristics of floc and the resistance forces ratio between permeable and impermeable floc (Ω), will be calculated with an appropriate empirical model. Namely a model will be selected which will predict sedimentation velocity based on particle permeability closest to the measured sedimentation velocity.

A generalized Stoke's model for terminal sedimentation velocity calculation (2) considers the force balance of the resistance force, the buoyancy and gravity:

$$v_s = \left[\frac{4g(\rho_k - \rho_l)d_k}{3\rho_l C_d} \right]^{\frac{1}{2}} \quad (2).$$

Several correlations have been developed for calculating C_d for $Re > 1$ and flocs of non-spherical shape, which thus induced us to carry-out comparative study [1]. Based on the results of this study, the Chien [12] model was selected for impermeable flocs within the range $0.2 \leq \psi \leq 1$ and $Re < \sim 5000$:

$$C_d = (30/Re) + 67.289 \cdot \exp^{-5.03\psi} \quad (3)$$

where the Re is calculated using the following expression:

$$Re = \frac{v_k \rho_k d_k}{\eta_i} \quad (4)$$

A floc consists of a large number of primary particles, having densities within the range $\rho_k < \rho_p < \rho_{ss}$ [10]. When the particles contain no liquid, then ρ_p equals ρ_{ss} [7] and [11], which does not hold in the case of activated sludge flocs. Therefore, in our case, we used the primary particle density ($\rho_p = 1059$ g/l), as defined by Li and Yuan [10].

The force balance for floc being porous ($\varepsilon > 0$) and permeable ($\Omega < 1$), and moving steadily, can be written as follows [5] and [13]:

$$\frac{\rho_k - \rho_l}{\rho_p - \rho_l} = 1 - \varepsilon = \frac{3\rho_l \Omega C_d}{4g(\rho_p - \rho_l)d_k} v_s^2 \quad (5)$$

Although the impact of permeability is often ignored [7] and [8], and (Ω) is set to 1, we decided to consider the permeability. Therefore, expression (5) was used to derive an expression for calculating sedimentation velocity based on porosity and permeability, which is as follows:

$$v_s = \sqrt{\frac{4g(\rho_p - \rho_l)(1 - \varepsilon)d_k}{3\rho_l \Omega C_d}} \quad (6)$$

For highly-porous spheres moving steadily through an infinite medium, the (Ω) factor can be calculated using the Brinkman model, as updated by Debye [4] and [13]:

$$\Omega = \frac{2\beta^2[1 - (\tanh(\beta))/\beta]}{2\beta^2 + 3[1 - (\tanh(\beta))/\beta]} \quad (7)$$

This is done using the permeability factor (β), which is a function of a floc's diameter and its permeability:

$$\beta = \frac{d_k}{2\sqrt{k}} \quad (8)$$

Permeability (k) has been calculated by various authors according to various models. Our

investigation tested those models proposed by Brinkman, Carman-Kozeny and Davies [4]:

$$\text{Brinkman } k = \frac{d_p^2}{72} \cdot \left(3 + \frac{4}{1 - \varepsilon} - 3\sqrt{\frac{8}{1 - \varepsilon} - 3}\right) \quad (9)$$

$$\text{Carman-Kozeny } k = \frac{\varepsilon^3}{5\left(\frac{6}{d_p}\right)^2(1 - \varepsilon)^2} \quad (10)$$

$$\text{Davies } k = \frac{d_p^2}{4} \cdot \frac{1}{16(1 - \varepsilon)^{3/2}(1 + (56(1 - \varepsilon)^3))} \quad (11)$$

3 FLOCS' FEATURES

3.1. Wastewater from the Lendava Biological Treatment Plant

This paper focuses on research results regarding sedimentation pool samples from the Lendava biological wastewater treatment plant (Slovenia). Wastewater samples were kept in a beaker, protected from air-inflow, for 1-3 days until performing dilution and analysis. The samples were kept at 20°C. The wastewater used during the analysis consisted of technological and municipal wastewaters in the ratio 75 : 25, the major part of the technological wastewater originating from the pharmaceutical industry. The municipal wastewater originated from the town of Lendava, and its surrounding villages.

3.2 Flocs' Shapes and Volumes

The shapes of flocs have been defined in previous studies [1], in which we estimated a 3D-shape of floc, having the face proportions of an equivalent cuboid. Our conclusion was that a floc can be approximated to a cuboid with faces in the ratios A : B : C = 1 : 0.89 : 0.69. By taking the A : B : C ratio into consideration, measurements of floc projections in plane A should suffice for estimating the remaining projected surfaces B and C, as well as the edges of the equivalent cuboid a , b and c . Thus we can simply estimate floc volume ($V = a \cdot b \cdot c$) and calculate the shape factor – the floc sphericity (ψ):

$$\psi = \frac{A_{\text{sphere}}}{A_k} \quad (12)$$

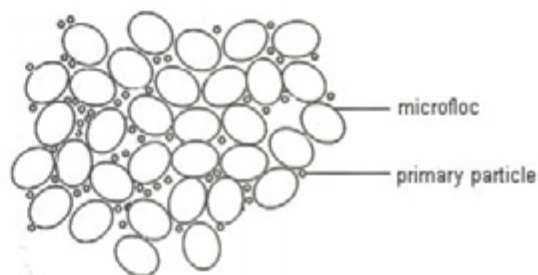


Fig 1. Floc's image (left) and its schematic sketch (right)

which is defined as the ratio of a sphere's surface area to the surface area of a floc with the same volume, and is used in expression (3) to calculate C_d . Sphericity, in our case, amounts to 0.796 and is very close to 0.8, the value defined by Tambo and Watanabe [7]. Figure 1 shows the grey image and schematic sketch of the floc, where its structure is evident.

It is clear from Fig. 1, that a floc consists of numerous smaller primary particles, which is emphasized in the schematic sketch of floc structure.

3.3. The Sizes of Primary Particles

The sizes of primary particles were defined using an AxioTech 25 HD (+pol) (ZEISS) stereoscopic microscope, an AxioCam MRc (D) high resolution microscopic camera with a digital interface and software (ZEISS), as well as KS 300 Rel. 3.0 image-analysis software with a supplement for true colour analysis (ZEISS). A freshly stirred (mixed for 2 hours at 600 rpm) and

diluted sample (1:20) was dripped on to a microscope's slide, covered with a cover slip (transmission microscopy) and analysed at a magnification of 500x (lit with a halogen lamp). Figure 2 shows the results of microscopy. An image analysis system was used to process the images. An appropriate threshold was selected for all the images taken, in order to convert them to binary images. This then enabled automatic processing, which eventually provided morphological features of the particles (the particle surface area and diameter in relation to the equivalent circle). The results of processing Fig. 2, are shown in Fig. 3, regarding particle size distribution. Fig. 2 shows some bigger particles with characteristic fractal floc structure ($d_p > 5 \mu\text{m}$), which were later ignored. Also, all particles smaller than $1 \mu\text{m}$ were omitted, as the microscope is intended for processing particles up to the size of $1 \mu\text{m}$. Thus, the resulting 70 particles rank among primary particles and have equivalent diameters between $1.077 \mu\text{m}$ and $4.746 \mu\text{m}$, see Fig. 4.

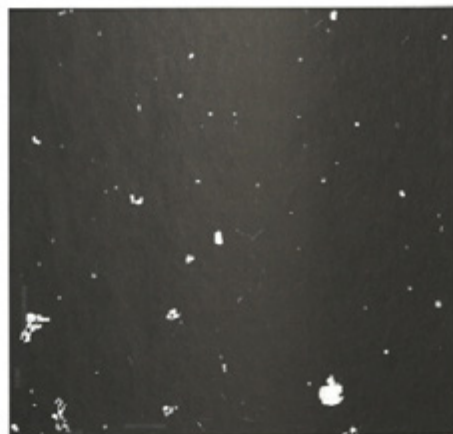
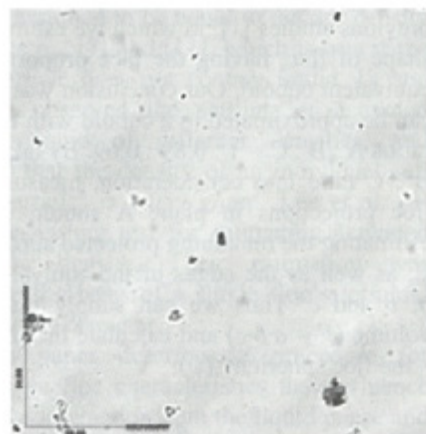


Fig. 2: Microscopic and binary images of primary particles

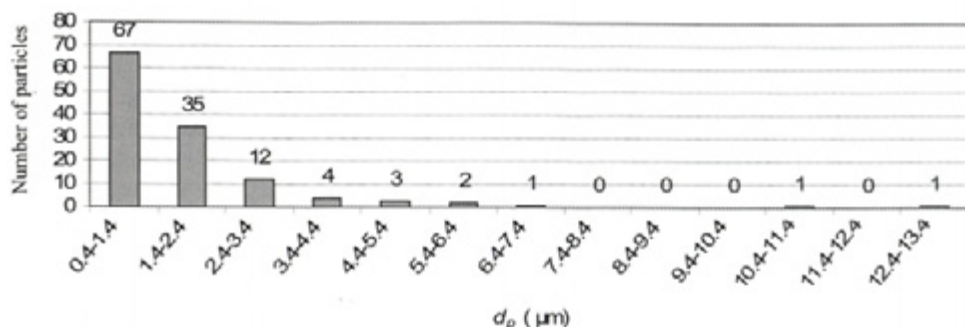


Fig.3. Particle size distribution for particles captured in Fig. 2

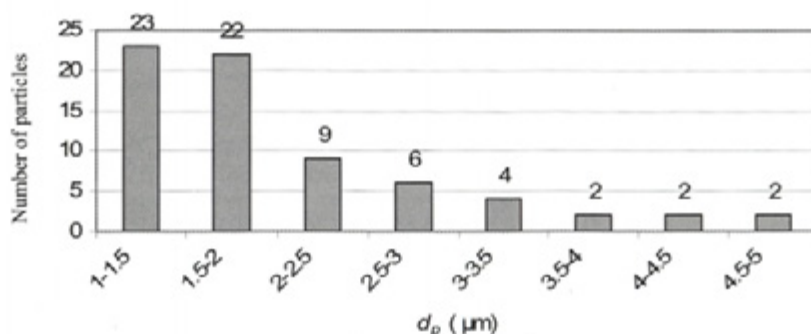


Fig. 4. Particle size distribution

It is evident that the majority of particles fall into the first two classes within sizes ranging from 1 μm to 2 μm , representing as much as 64.3 % of all particles.

The average diameter of all particles from Fig. 2 is 2.019 μm , which can be considered the average equivalent primary particle diameter. This value falls within the size range of primary particles (1 μm -20 μm), as stated by other authors [2], [4] to [6] and [11].

3.4 Sizes and Velocities of Floc Sedimentation

Sedimentation velocity was measured by dropping small amounts (drops) of a previously diluted sample (1:1) at 20°C into a glass tower of size 330 x 260 x 60 mm, filled with distilled water, where the floc freely sedimented. A camera was used to shoot flocs sedimentation at a depth of 230 mm.

The Nikon Hi Sence camera was used which takes shots of floc movements over set time-intervals. Images were processed using special software written in Java language, which determines

position (coordinates x and y) and sizes – surfaces of each floc on the image. With a procession of successive images we can calculate the speeds of flocs and determine their route through the observed area. The time-interval between shots can be set, in our case 0.75 s. The software also computes the size – surface areas of flocs (2D projection) on the images, which is used to calculate the equivalent diameters of flocs.

The results for individual free-settling tests were merged and any change in deviation (σ) monitored by increasing the number of measurements. As evident from Fig. 5, σ decreases with the number of flocs and settles when $n > 250$. It can be assumed, with sufficient probability, that this is the lower size limit of the representative sample when defining the sizes of flocs, as well as the sedimentation velocity.

The whole sample processed by the presented method consists of 307 flocs. Their diameter ranges between 0.147 mm and 1.736 mm. Floc size distribution is presented in Fig. 6.

It is evident from Fig. 6 that the first, second and third class sizes with floc size ranging from

0.147 to 0.676 mm comprise the majority of flocs, while later on the number of flocs decreases.

Fig. 7 shows the measured velocities of the 307 flocs observed. It shows the comparison between the measured sedimentation velocities (v_k) and those velocities predicted by the general Stokes model (v_s) (Eq. 6), and by considering the drag coefficient C_d according to Chien (Eq.3) [12], the constant porosity ($\epsilon = 0.977$) according to Li and Yuan [10] and the assumption of impermeable floc (the resistance forces ratio between permeable and impermeable floc ($\Omega=1$)) [4], [7]).

The measured velocity of a floc's sedimentation increases with diameter, which agrees with the results of other authors [4]. However, there is a difference between measured and calculated velocities, which is due to having applied constant floc porosities. The porous structure of flocs has a direct impact on floc density and a floc's resistance force. Further research was carried-out to observe this phenomenon and improve the empirical model for predicting the terminal velocity of floc sedimentation.

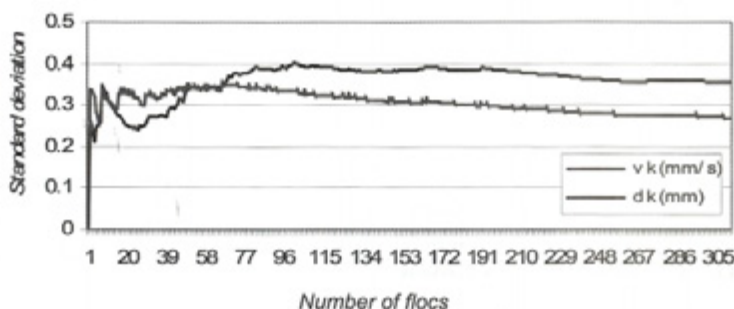


Fig. 5. Variations in the standard deviation diameters of flocs, as presented by the observed flocs

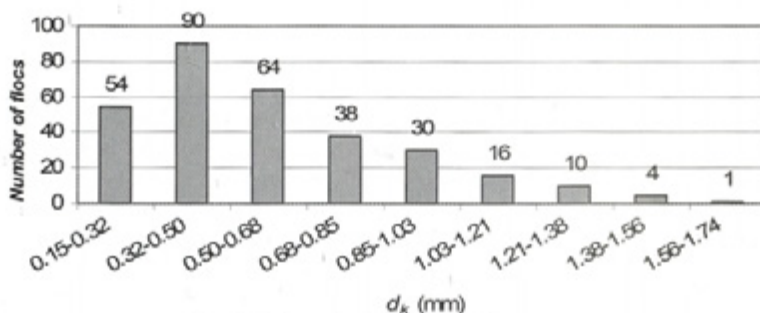


Fig. 6. Size distribution of flocs

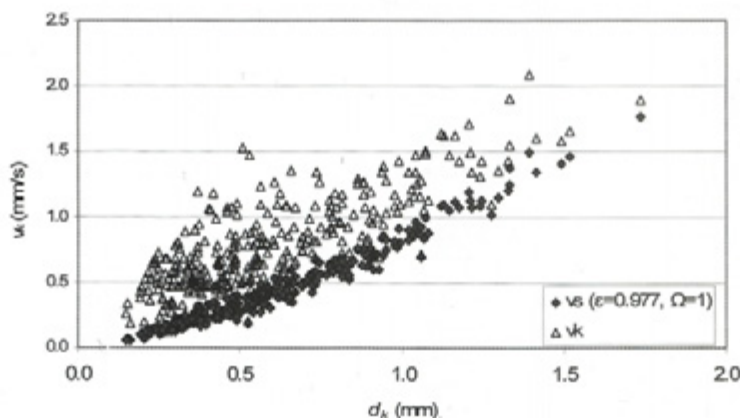


Fig. 7. Measured velocities of flocs (v_k) in comparison with those velocities predicted using the general Stokes model (v_s) (Eq. 2)

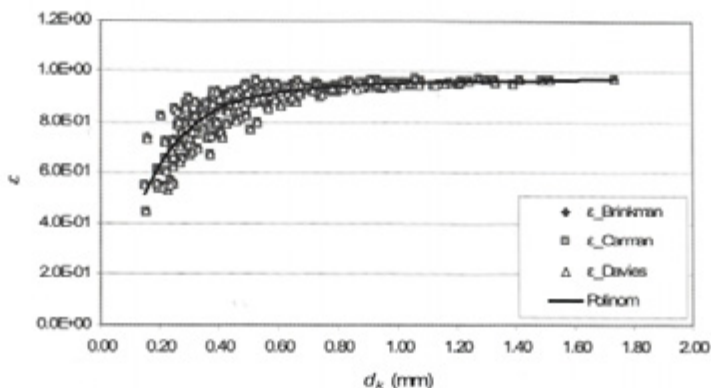


Fig. 8. The porosities of flocs calculated using permeability models: Brinkman, Carman-Kozeny and Davies

3.5. Permeability of porous flocs

In order to consider permeability when calculating sedimentation velocity the following models of permeability were used: (Eq. 9), (Eq. 10) and (Eq. 11). Interdependence between porosity (ε) and permeability (k) was considered when calculating the resistance forces ratio of permeable and impermeable flocs (Ω) (Eq. 7).

Combining expressions (5) and (7-11), in principle, enables the following to be stated:

$$1 - \varepsilon = \frac{3\rho_f \Omega(\beta(k(d_p, \varepsilon)), d_k) C_d}{4g(\rho_p - \rho_f) d_k} v_s^2 \quad (13)$$

The expression (13) was evaluated iteratively for each of the 307 flocs previously measured considering their sedimentation velocities and equivalent diameters (Fig. 7). All the three presented models were used to calculate porosity and permeability $k(d_p, \varepsilon)$. Fig. 8 shows the calculated values for porosities.

The results show that porosity increases with the increase in floc diameter. From 1 mm onwards, porosity does not change significantly. We also observed that the predicted trend regarding porosity, depending on floc diameter, is not influenced by the model used for calculating permeability. Any changes in porosity do not exceed 1%. For the simple calculation of porosity, we therefore derived the average regression polynomial valid within the range 0.2 to 1.8 mm, and acquired on the basis of all three sets of results:

$$\begin{aligned} \varepsilon = & -0.53d_k^6 + 3.61d_k^5 - 10.01d_k^4 \\ & + 14.52d_k^3 - 11.74d_k^2 \\ & + 5.14d_k - 0.03 \end{aligned} \quad (14)$$

The expression for floc porosity, defined in such a way, has been put into expressions for permeability (9) to (11). Fig. 9 presents permeability values calculated in this manner.

In contrast to porosity, the permeability of flocs does differ when using different models, which is particularly evident for larger flocs. Yet all three models show the same trend, which is an increase in permeability with any increase in floc size, a result also observed by other authors [4].

Absolute permeability values are very small, typically about 10^{-12} m^2 which means, that the flow of liquid through a floc is very slow. In regard to the fact that the velocities of moving flocs by sedimentation are relatively large, we can conclude that the influence of permeability on the change of velocity during sedimentation is small.

Fig. 10 shows the permeability factor (β), representing the ratio between floc diameter and permeability. As it turns out, the permeability factor is the largest with small flocs ($d_k < 0.5 \text{ mm}$) and then decreases, only to become independent of floc size for large flocs.

After calculating the permeability factor (β), Eq. (7) was used to calculate resistance forces ratio between permeable and impermeable floc (Ω), which has a direct impact on floc sedimentation velocity (Eq. (6)) and thus enables

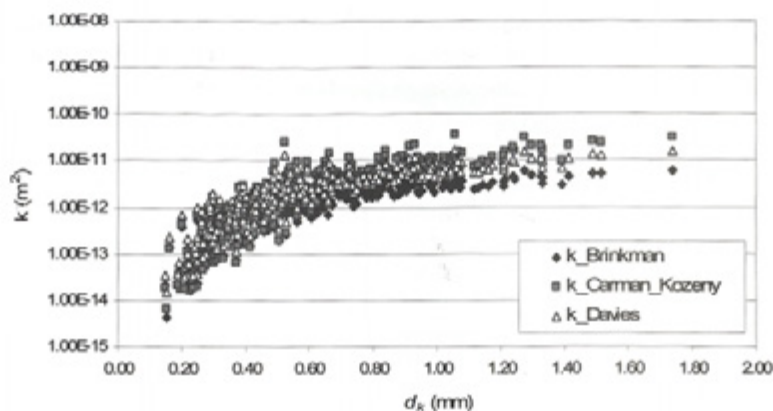


Fig. 9. Floc permeability according to models: Brinkman, Carman-Kozeny and Davies

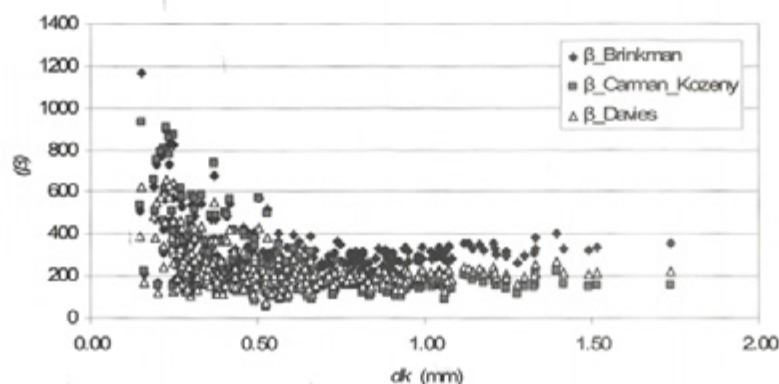


Fig. 10. Permeability factor (β) according to permeability models: Brinkman, Carman-Kozeny and Davies

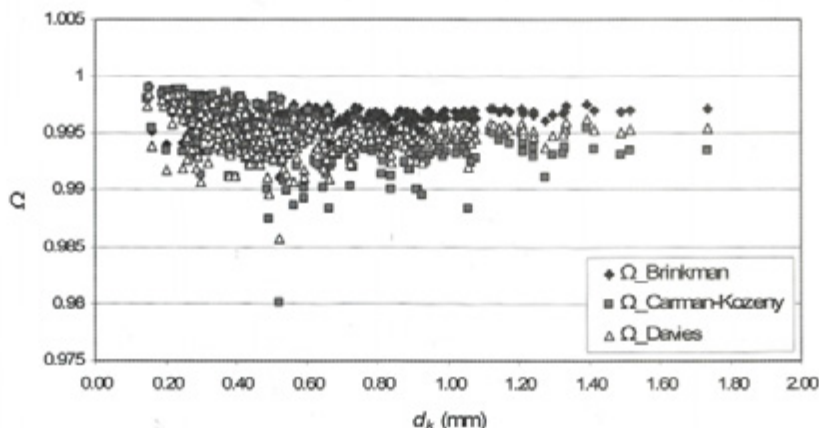


Fig. 11. Resistance forces ratio between permeable and impermeable flocs (Ω) using permeability models: Brinkman, Carman-Kozeny and Davies

evaluation of the importance of permeability for floc sedimentation. The dependence of factor (Ω) on the choice of a permeability model is shown in Fig. 11. The resistance force ratio between permeable and impermeable flocs (Ω) is close to the value of 1 for all three permeability models. The highest impact on (Ω) when increasing floc diameter is shown by the Carman-Kozeny permeability model, which was developed for primary particles of spherical shape. A high impact on (Ω) is also evident when observing the Davies permeability model, which was developed for fibrous primary particles. The lowest impact of floc size on (Ω) appears when using the Brinkman permeability model. Despite of a slight deviation of (Ω) values between various permeability models, low permeabilities mean that the velocity of liquid through the floc is very low in all cases, and can thus be ignored, which is also true for floc permeability, confirming the result of some authors [9], [13].

3.6. Floc density

Floc density has been derived from expression (5) and is as follows:

$$\rho_k = \rho_l + (1 - \varepsilon)(\rho_p - \rho_l) \quad (15)$$

With known liquid density, the calculated floc porosity and the defined density of the primary particle 1.059 g/cm^3 [10], we used expression (15) to calculate the floc density. Fig. 12 shows the results of density differences between floc and liquid (16).

$$\Delta\rho = \rho_k - \rho_l \quad (16)$$

It is evident that smaller flocs have higher densities than larger flocs, which is in line with the findings by Lee et al. [4] who observed a decrease in value $\Delta\rho$ from 100 to 0.1 kg/m^3 with any increase in floc diameter from 0.1 mm to 10 mm . The density differences can change according to the wastewater composition and type of BTW.

For the results within the same sample from selected BTW the difference in density (Fig. 12) is a consequence of varying floc porosity. Big flocs with large porosities have smaller differences in densities than small flocs, which are more compact.

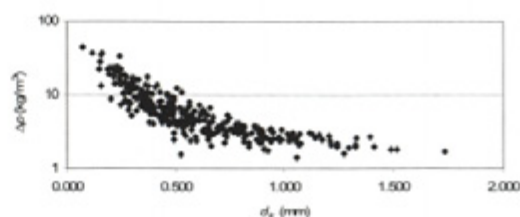


Fig. 12. A presentation of differences between floc and liquid densities depending on floc diameter

4 CONCLUSIONS

A detailed study of sedimentation of wastewater sludge flocs was performed. Based on the measured velocities of sedimentation for various sizes of flocs and the use of a generalized Stokes' model for sedimentation velocity, we derived values for flocs' porosities, considering that the flocs are permeable and composed of smaller primary particles.

Experimental results and obtained empirical correlations demonstrate that porosity values of flocs increase with their size (equal diameter). With increasing the size of a floc the difference between the floc's density and the liquid (water) density decreases. From the main findings, i.e. low values of permeability, we conclude, that in practice the influence of the liquid flow through the porous floc can in most cases be neglected.

On the other hand, developed correlations for the floc porosity and permeability can be used in deriving a suitable numerical model for sedimentation of sludge flocs, which is the next step in modelling of the sedimentation process.

5 NOMENCLATURE

| | | |
|---------------|-------------------|---|
| C_d | | drag coefficient |
| g | mm/s ² | gravitational acceleration |
| d_k | mm | floc diameter |
| d_p | mm | primary particle diameter |
| v_s | mm/s | settling velocity of floc predicted by Stokes' law |
| v_k | mm/s | settling velocity of floc (measured) |
| v_l | mm/s | velocity of fluid |
| ε | | porosity |
| k | mm ² | permeability |
| ψ | | sphericity |
| m_k | g | floc mass |
| ρ_k | g/mm ³ | floc density |
| ρ_l | g/mm ³ | fluid density |
| ρ_p | g/mm ³ | primary particle density |
| ρ_{ss} | g/mm ³ | dry density of floc |
| η_l | g/mms | dynamic viscosity |
| $\Delta\rho$ | g/mm ³ | differences in floc and liquid density |
| Ω | | the ratio of the resistance of permeable and impermeable floc |
| β | | dimensionless permeability factor |
| A_k | mm ² | surface area of floc |
| A_{krogle} | mm ² | surface area of equivalent sphere |
| A, B, C | mm ² | projection areas of equivalent cuboid |
| a, b, c | mm | edges of equivalent cuboid |

6 REFERENCES

- [1] Žajdela, B., Hribernik, A., Hriberšek, M. Experimental investigations of sedimentation of flocs in suspensions of biological water treatment plants, *Computation methods in multiphase flow*, 2007, IV, pp. 293-302.
- [2] Li, D.-H. & Ganczarczyk, J. J. Advective transport in activated sludge flocs, *Wat. Env. Res.*, 1992, 64, pp. 236-240.
- [3] Li, D.-H. & Ganczarczyk, J. J. Stroboscopic determination of settling velocity, size and porosity of activated sludge flocs, *Wat. Res.*, 1987, 21, pp. 257-262.
- [4] Lee, D. J., Chen, G. W. & Hsieh, C. C. On the free-settling test for estimating activated sludge floc density, *Wat. Res.*, 1996, 30, pp. 541-550.
- [5] Huang, H. Porosity - size relationship of drilling mud flocs: fractal structure, *Clay Miner.*, 1993, 41, pp. 373-379.
- [6] Jorand, F., Zartarian, F., Block, J.C., Bottero J. Y., Villemin, G., Urbain, V., Manem, J. Chemical and structural (2D) linkage between bacteria within activated sludge flocs, *Wat. Res.*, 1995, 29, pp. 1639-1647.
- [7] Tambo, N. & Watanabe, Y. Physical characteristics of flocs. 1. The floc density function and aluminum floc, *Wat. Res.*, 1979, 13, pp. 409-419.
- [8] Concha, F. & Almerdra, E. R. Settling velocities of particulate system, 1. Settling velocities of individual spherical particles, *Int. J. Min. Process.*, 1979, 5, pp. 349-367.
- [9] Matsumoto, K., Sukanuma, K. Settling velocity of a permeable model floc, *Chem. Engng.*, 1977, 32, pp. 445-447.
- [10] Li, X., Yuan, Y. Settling velocities and permeabilities of microbial aggregates, *Wat. Res.*, 2002, 36, pp. 3110-3120.
- [11] Li, D.-H. & Ganczarczyk, J. J., Size distribution of activated sludge flocs, *Res. Jour. WPCF.*, 1991, 63, pp. 806-814.
- [12] Chien, S. F. Settling velocity of irregularly shaped particles, *SPE Drilling and Completion*, 1994, pp. 281-289.
- [13] Neale, G., Epstein, N. & Nader, W. Creeping flow relative to permeable spheres, *Chem. Engng.*, 1973, 28, pp. 1865-1874.
- [14] Crowe, C., Sommerfeld, M., Tsuji, Y. Multiphase flow whit droplets and particles, *CRC Press*, 1998, pp. 92-93.